Computers and Concrete, *Vol. 26, No. 1 (2020) 21-30*
DOI: https://doi.org/10.12989/cac.2020.26.1.021

Post-buckling analysis of geometrically imperfect nanoparticle reinforced annular sector plates under radial compression

Seyed Sajad Mirjavadi[1], Masoud Forsat*[1], Saeed Mollaee[2], Mohammad Reza Barati[3], Behzad Mohasel Afshari[4] and A.M.S. Hamouda[1]

[1]*Department of Mechanical and Industrial Engineering, Qatar University, P.O. Box 2713, Doha, Qatar*
[2]*Auckland Bioengineering Institute, the University of Auckland, Auckland, New Zealand*
[3]*Fidar Project Qaem Company, Darvazeh Dolat, Tehran, Iran*
[4]*School of Mechanical Engineering, College of Engineering, Sharif University of Technology, Tehran, Iran*

(*Received February 4, 2020, Revised May 26, 2020, Accepted May 29, 2020*)

Abstract. Buckling and post-buckling behaviors of geometrically imperfect annular sector plates made from nanoparticle reinforced composites have been investigated. Two types of nanoparticles are considered including graphene oxide powders (GOPs) and silicone oxide (SiO_2). Nanoparticles are considered to have uniform and functionally graded distributions within the matrix and the material properties are derived using Halpin-Tsai procedure. Annular sector plate is formulated based upon thin shell theory considering geometric nonlinearity and imperfectness. After solving the governing equations via Galerkin's technique, it is showed that the post-buckling curves of annular sector plates rely on the geometric imperfection, nanoparticle type, amount of nanoparticles, sector inner/outer radius and sector open angle.

Keywords: post-buckling; thin shell theory; nanoparticles; graphene oxide powder; nonlinear stability

1. Introduction

Based on recent developments, a variety of carbon based structures containing carbon nanotube or carbon fiber have been widely utilized in composites for enhancing their mechanics and thermal specifications (Zhang 2017, Keleshtreri *et al*. 2016, Belbachir *et al*. 2019, Draoui *et al*. 2019, Medani *et al*. 2019). A 273% enhancement of elastic modulus is obtained by Ahankari *et al*. (2010) for carbon reinforced composites in comparison to conventional composites. Likewise, Gojny *et al*. (2004) mentioned that structural stiffness of carbon based composites may be enhanced with incorporation of carbon nanotube within material. Impacts of configuration and scale of carbon nanotubes on rigidity growth of material composites having metallic matrices are studied by Esawi *et al*. (2011). Because of possessing above mentioned properties, beam and plate structures having carbon based fillers are researched to understand their static or dynamical status (Yang *et al*. 2017, Semmah *et al*. 2019, Hussain *et al*. 2019). There are also some investigations on composite or functionally graded materials and interested readers are refaced to new investigations on materials (Barati and Zenkour 2018, Shafiei *et al*. 2017, Mirjavadi *et al*. 2017, 2018, 2019, Azimi *et al*. 2017, 2018, Hellal *et al*. 2019, Tlidji *et al*. 2019, Chaabane *et al*. 2019, Keddari *et al*. 2020, Berghouti *et al*. 2019, Bourada *et al*. 2019, Sahla *et al*. 2019, Boutaleb *et al*. 2019, Boulefrakh *et al*. 2019, Boukhlif *et al*. 2019, Boussoula *et al*. 2020, Bellal *et al*. 2020). Furthermore, the graphene based composite material has been recently gained enormous attentions because of having easy producing procedure and high rigidity growth. Nieto *et al*. (2017) presented a review paper based on several graphene based composite material possessing ceramic or metallic matrices. The multi-scale study of mechanical attributes for graphene based composite material has been provided by Lin *et al*. (2018) utilizing finite elements approach.

Until now, many of researches in the fields of nano-composites have been interested in production and materials characteristics recognition of graphene based composites and structural components containing slight percentages of graphene fillers. For instance, it is mentioned by Rafiee *et al*. (2009) that some material characteristics of graphene based composites may be enhanced via placing 0.1% volume of graphene filler. However, achieving to this level of reinforcement employing nanotubes required 1% of their volume. Graphene based composites containing epoxy matrix were created by King *et al*. (2013) by placing 6% weight fraction of graphene fillers to polymeric phases. It was stated that Young modulus of the composite has been increased from 2.72 GPa to 3.36 GPa. Next, 57% increment for Young modulus has been achieved by Fang *et al*. (2009) based on a sample of graphene based composite.

Moreover, many studies in the fields of nano-mechanic are associated with vibrational and stability investigation of various structural elements containing beam or plate reinforced via diverse graphene dispersions. For instance, vibrational properties of a laminated graphene based plate have been explored by Song *et al*. (2017) assuming simply support edge condition. They assumed that the plate is

*Corresponding author, Ph.D.
E-mail: masoudforsatlar@gmail.com

http://www.techno-press.org/?journal=cac&subpage=8
ISSN: 1598-8198 (Print), 1598-818X (Online)

constructed from particular numbers of layers each containing a sensible content of graphene. Selecting a perturbation approach, static deflections and bucking loads of graphene based plates have been derived by Shen *et al*. (2017). In above papers, each material property has discontinuous variation across the thickness of beam or plate. Also, geometrically nonlinear vibration frequencies of graphene based beams having embedded graphene have been explored by Feng *et al.* (2017) selecting first-order beam theory. Moreover, vibration frequencies of graphene based beams having porosities have been explored by Kitipornchai *et al*. (2017).

Furthermore, reinforcement of matrix materials with nano-size inclusions is a novel case study (Alijani and Bidgoli 2018, Guenaneche *et al*. 2019, Zaheer *et al*. 2019, Alimirzaei *et al*. 2019). Many researches show that mechanical properties of concrete can be enhanced by adding graphene platelets (GPLs), graphene oxide powders (GOPs) and ever carbon nanotubes (Du *et al*. 2016, Shamsaei *et al*. 2018). Graphene oxide, as derivative of graphene, is broadly and economically available from graphite mass oxidations. It is compatible with many matix materials including polymeric materials and even concrete (Mohammed *et al*. 2017). Graphene oxide composite exhibits great Young modulus and tensile strength as are carbon-based material with remarkable performances and low costs (Zhang *et al*. 2020). To the best of author's knowledge, post-buckling study of geometrically imperfect (Wang *et al*. 2018) annular sector plates reinforced by nanoparticles is not carried out till to now.

In this article, post-buckling behaviors of geometrically imperfect annular sector plates made from nanoparticle reinforced composites have been investigated. Two types of nanoparticles are considered including graphene oxide powders (GOPs) and silicone oxide (SiO_2). Nanoparticles are considered to have uniform and graded distributions within the matrix and the material properties are derived using Halpin-Tsai procedure. Annular sector plate is formulated based upon thin shell theory considering geometric nonlinearity and imperfectness. After solving the governing equations via Galerkin's technique, it is showed that the post-buckling curves of annular sector plates rely on the geometric imperfection, nanoparticle type, amount of nanoparticles, sector inner/outer radius and sector open angle.

2. Nanoparticle reinforced composites

Two types of nanoparticles are considered including graphene oxide powders (GOPs) and silicone oxide (SiO_2). Micro-mechanic theory of such composite materials (Liew *et al*. 2015) introduces the below relationship between nanoparticles weight fraction ($W_{particle}$) and their volume fraction ($V_{particle}$) by

$$V^*_{particle} = \frac{W_{particle}}{W_{particle} + \frac{\rho_{particle}}{\rho_M} - \frac{\rho_{particle}}{\rho_M} W_{particle}} \tag{1}$$

where $\rho_{particle}$ and ρ_M define the mass densities of nanoparticle and matrices, respectively. Next, the elastic modulus of a nanoparticle based composite might be represented based upon matrix elastic modulus (E_M) by (Zhang *et al*. 2020)

$$\begin{aligned} E_1 &= 0.49\left(\frac{1+\xi_L^{particle}\eta_L^{particle}V_{particle}}{1-\eta_L^{particle}V_{particle}}\right)E_M \\ &+0.51\left(\frac{1+\xi_W^{particle}\eta_W^{particle}V_{particle}}{1-\eta_W^{particle}V_{particle}}\right)E_M \end{aligned} \tag{2}$$

so that $\xi_L^{particle}$ and $\xi_W^{particle}$ define two geometrical factors indicating the impacts of nanoparticle configuration and scales as

$$\xi_L^{particle} = \frac{2d_{particle}}{t_{particle}} \tag{3a}$$

$$\eta_L^{particle} = \frac{\left(E_{particle}/E_M\right)-1}{\left(E_{particle}/E_M\right)+\xi_L^{particle}} \tag{3b}$$

$$\xi_W^{particle} = \frac{2d_{particle}}{t_{particle}} \tag{3c}$$

$$\eta_W^{particle} = \frac{\left(E_{particle}/E_M\right)-1}{\left(E_{particle}/E_M\right)+\xi_W^{particle}} \tag{3d}$$

so that $d_{particle}$ and $t_{particle}$ define nanoparticle average diameter and thickness, respectively. Furthermore, Poisson's ratio for nanoparticle based composite might be defined based upon Poisson's ratio of the two constituents in the form

$$v_1 = v_{particle}V_{particle} + v_M V_M \tag{4}$$

in which $V_M=1-V_{particle}$ expresses the volume fractions of matrix component (Metwally *et al*. 2014). Herein, three dispersions of the nanoparticle have been assumed as

$$V_{particle} = \begin{cases} V^*_{particle} & \text{(UD)} \\ 2V^*_{particle}\left(1-\frac{2|z|}{h}\right) & \text{(FG-O)} \\ 4V^*_{particle}\frac{|z|}{h} & \text{(FG-X)} \end{cases} \tag{5}$$

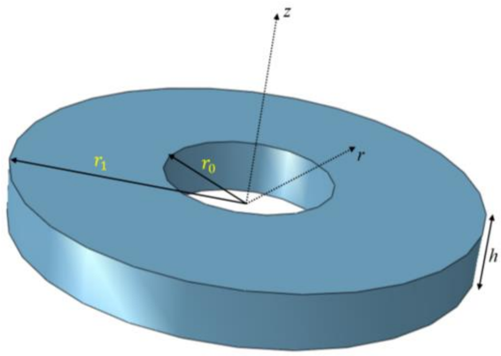

Fig. 1 Geometry of the annular plate

3. Derivation of equations of motion

Considering inner radius (r_0), outer radius (r_1) and open angel (ψ), Fig. 1 illustrates the geometry of an annular sector plate. As mentioned, the annular sector is made of nanoparticle reinforced composite material for which the stresses σ_p (p=r, φ, $r\varphi$) can be determined as

$$\begin{Bmatrix} \sigma_r \\ \sigma_\varphi \\ \sigma_{r\varphi} \end{Bmatrix} = \begin{pmatrix} Q_{11} & Q_{12} & 0 \\ Q_{12} & Q_{22} & 0 \\ 0 & 0 & Q_{66} \end{pmatrix} \begin{Bmatrix} \varepsilon_r \\ \varepsilon_\varphi \\ \gamma_{r\varphi} \end{Bmatrix} \tag{6}$$

in which

$$Q_{11} = Q_{22} = \frac{E_1}{1-\nu_1^2}, \quad Q_{12} = \frac{\nu_1 E_1}{1-\nu_1^2}, \quad Q_{66} = \frac{E_1}{2(1+\nu_1)} \tag{7}$$

For a thin annular sector plate, components of strain field considering imperfection deflection (w^*) are (Barati and Zenkour 2019)

$$\begin{aligned} \varepsilon_r &= \varepsilon_r^0 - z\chi_r, \\ \varepsilon_\varphi &= \varepsilon_\varphi^0 - z\chi_\varphi, \\ \gamma_{r\varphi} &= \gamma_{r\varphi}^0 - 2z\chi_{r\varphi}. \end{aligned} \tag{8}$$

in which

$$\begin{aligned} \varepsilon_r^0 &= \frac{\partial u}{\partial r} + \frac{1}{2}\left(\frac{\partial w}{\partial r}\right)^2 + \frac{\partial w}{\partial r}\frac{\partial w^*}{\partial r}, \\ \varepsilon_\varphi^0 &= \frac{1}{r}\left(\frac{\partial v}{\partial \varphi} + u\right) + \frac{1}{2r^2}\left(\frac{\partial w}{\partial \varphi}\right)^2 + \frac{1}{r^2}\frac{\partial w}{\partial \varphi}\frac{\partial w^*}{\partial \varphi}, \\ \gamma_{r\varphi}^0 &= \frac{\partial v}{\partial r} - \frac{v}{r} + \frac{1}{r}\frac{\partial u}{\partial \varphi} + \frac{1}{r}\frac{\partial w}{\partial r}\frac{\partial w}{\partial \varphi} + \frac{1}{r}\frac{\partial w^*}{\partial r}\frac{\partial w}{\partial \varphi} + \frac{1}{r}\frac{\partial w}{\partial r}\frac{\partial w^*}{\partial \varphi}, \\ \chi_r &= \frac{\partial^2 w}{\partial r^2}, \quad \chi_\varphi = \frac{1}{r}\frac{\partial w}{\partial r} + \frac{1}{r^2}\frac{\partial^2 w}{\partial \varphi^2}, \quad \chi_{r\varphi} = \frac{1}{r}\frac{\partial^2 w}{\partial r \partial \varphi} - \frac{1}{r^2}\frac{\partial w}{\partial \varphi} \end{aligned} \tag{9}$$

Sector deflection is denoted by w and in-plane displacements are denoted by u and v. Annular sector plate contains stresses which result in below forces and moments via integrating Eq. (6) over sector thickness

$$\begin{aligned} \begin{Bmatrix} N_r \\ N_\varphi \\ N_{r\varphi} \end{Bmatrix} &= \begin{pmatrix} A_{11} & A_{12} & 0 \\ A_{12} & A_{22} & 0 \\ 0 & 0 & A_{66} \end{pmatrix} \begin{Bmatrix} \varepsilon_r^0 \\ \varepsilon_\varphi^0 \\ \gamma_{r\varphi}^0 \end{Bmatrix} \\ &- \begin{pmatrix} B_{11} & B_{12} & 0 \\ B_{12} & B_{22} & 0 \\ 0 & 0 & B_{66} \end{pmatrix} \begin{Bmatrix} \chi_r \\ \chi_\varphi \\ 2\chi_{r\varphi} \end{Bmatrix} \end{aligned} \tag{10}$$

$$\begin{aligned} \begin{Bmatrix} M_r \\ M_\varphi \\ M_{r\varphi} \end{Bmatrix} &= \begin{pmatrix} B_{11} & B_{12} & 0 \\ B_{12} & B_{22} & 0 \\ 0 & 0 & B_{66} \end{pmatrix} \begin{Bmatrix} \varepsilon_r^0 \\ \varepsilon_\varphi^0 \\ \gamma_{r\varphi}^0 \end{Bmatrix} \\ &- \begin{pmatrix} D_{11} & D_{12} & 0 \\ D_{12} & D_{22} & 0 \\ 0 & 0 & D_{66} \end{pmatrix} \begin{Bmatrix} \chi_r \\ \chi_\varphi \\ 2\chi_{r\varphi} \end{Bmatrix} \end{aligned} \tag{11}$$

in which

$$\begin{aligned} &A_s = \int_{-h/2}^{h/2} Q_s dz, \quad B_s = \int_{-h/2}^{h/2} Q_s z dz, D_s = \int_{-h/2}^{h/2} Q_s z^2 dz, \\ &s = \{11, 12, 22, 66\} \end{aligned} \tag{12}$$

Finally, one may express the governing equations for an annular sector plate as

$$\frac{\partial N_r}{\partial r} + \frac{1}{r}\frac{\partial N_{r\theta}}{\partial \theta} + \frac{1}{r}(N_r - N_\theta) = 0 \tag{13}$$

$$\frac{\partial N_{r\theta}}{\partial r} + \frac{1}{r}\frac{\partial N_\theta}{\partial \theta} + \frac{2}{r}N_{r\theta} = 0 \tag{14}$$

$$\begin{aligned} &\frac{\partial^2 M_r}{\partial r^2} + \frac{2}{r}\frac{\partial M_r}{\partial r} + \frac{2}{r}\frac{\partial^2 M_{r\theta}}{\partial r \partial \theta} + \frac{2}{r^2}\frac{\partial M_{r\theta}}{\partial \theta} \\ &+ \frac{1}{r^2}\frac{\partial^2 M_\theta}{\partial \theta^2} - \frac{1}{r}\frac{\partial M_\theta}{\partial r} + N_r\left(\frac{\partial^2 w}{\partial r^2} + \frac{\partial^2 w^*}{\partial r^2}\right) \\ &- 2N_{r\theta}\left[\frac{1}{r^2}\left(\frac{\partial w}{\partial \theta} + \frac{\partial w^*}{\partial \theta}\right) - \frac{1}{r}\left(\frac{\partial^2 w}{\partial r \partial \theta} + \frac{\partial^2 w^*}{\partial r \partial \theta}\right)\right] \\ &+ N_\theta\left[\frac{1}{r}\left(\frac{\partial w}{\partial r} + \frac{\partial w^*}{\partial r}\right) + \frac{1}{r^2}\left(\frac{\partial^2 w}{\partial \theta^2} + \frac{\partial^2 w^*}{\partial \theta^2}\right)\right] \\ &- P_r\left(\frac{\partial^2 w}{\partial r^2} + \frac{\partial^2 w^*}{\partial r^2}\right) = 0 \end{aligned} \tag{15}$$

where P_r is radial load. By substituting Eqs. (10)-(11) into Eqs. (13) and (15), nonlinear governing equations in terms of strain components can be simply expressed in compact forms

$$\begin{aligned} &\frac{\partial}{\partial r}[A_{11}\varepsilon_r^0 + A_{12}\varepsilon_\varphi^0 - B_{11}\chi_r - B_{21}\chi_\varphi] \\ &+ \frac{1}{r}\frac{\partial}{\partial \theta}[A_{66}\gamma_{r\varphi}^0 - 2B_{66}\chi_{r\varphi}] \\ &+ \frac{1}{r}(A_{11}\varepsilon_r^0 + A_{12}\varepsilon_\varphi^0 - B_{11}\chi_r - B_{21}\chi_\varphi \\ &- A_{12}\varepsilon_r^0 - A_{22}\varepsilon_\varphi^0 + B_{12}\chi_r + B_{22}\chi_\varphi) = 0 \end{aligned} \tag{16}$$

$$\begin{aligned} &\frac{\partial}{\partial r}[A_{66}\gamma_{r\varphi}^0 - 2B_{66}\chi_{r\varphi}] \\ &+ \frac{1}{r}\frac{\partial}{\partial \theta}[A_{12}\varepsilon_r^0 + A_{22}\varepsilon_\varphi^0 - B_{12}\chi_r - B_{22}\chi_\varphi] \\ &+ \frac{2}{r}[+A_{66}\gamma_{r\varphi}^0 - 2B_{66}\chi_{r\varphi}] = 0 \end{aligned} \tag{17}$$

$$\begin{aligned} &\left(\frac{\partial^2}{\partial r^2} + \frac{2}{r}\frac{\partial}{\partial r}\right)[B_{11}\varepsilon_r^0 + B_{12}\varepsilon_\varphi^0 - D_{11}\chi_r + D_{12}\chi_\varphi] \\ &+ \left(\frac{2}{r}\frac{\partial^2}{\partial r \partial \theta} + \frac{2}{r^2}\frac{\partial}{\partial \theta}\right)[B_{66}\gamma_{r\varphi}^0 - 2D_{66}\chi_{r\varphi}] \\ &+ \frac{1}{r^2}\frac{\partial^2}{\partial \theta^2}[B_{12}\varepsilon_r^0 + B_{22}\varepsilon_\varphi^0 - D_{12}\chi_r - D_{22}\chi_\varphi] \\ &- \frac{1}{r}\frac{\partial}{\partial r}[B_{12}\varepsilon_r^0 + B_{22}\varepsilon_\varphi^0 - D_{12}\chi_r - D_{22}\chi_\varphi] \end{aligned}$$

$$
\begin{aligned}
&+[A_{11}\varepsilon_r^0 + A_{12}\varepsilon_\varphi^0 - B_{11}\chi_r - B_{21}\chi_\varphi](\frac{\partial^2 w}{\partial r^2} + \frac{\partial^2 w^*}{\partial r^2}) \\
&-2[A_{66}\gamma_{r\varphi r}^0 - 2B_{66}\chi_{r\varphi}] \\
&[\frac{1}{r^2}(\frac{\partial w}{\partial \theta} + \frac{\partial w^*}{\partial \theta}) - \frac{1}{r}(\frac{\partial^2 w}{\partial r \partial \theta} + \frac{\partial^2 w^*}{\partial r \partial \theta})] \\
&+[A_{12}\varepsilon_r^0 + A_{22}\varepsilon_\varphi^0 - B_{12}\chi_r - B_{22}\chi_\varphi] \\
&[\frac{1}{r}(\frac{\partial w}{\partial r} + \frac{\partial w^*}{\partial r}) + \frac{1}{r^2}(\frac{\partial^2 w}{\partial \theta^2} + \frac{\partial^2 w^*}{\partial \theta^2})] \\
&-P_r(\frac{\partial^2 w}{\partial r^2} + \frac{\partial^2 w^*}{\partial r^2}) = 0
\end{aligned} \tag{18}
$$

4. Method of solution

Presented in this chapter is numerical solution of the non-linear governing equations for post-buckling of a nanoparticle-reinforced annular plate. The below edge conditions may be introduced for mechanical post-buckling analyzes of simply-supported plate as

$$
\begin{aligned}
&w = M_r = N_{r\theta} = 0 \ \text{ at } r=r_0, r=r_1 \\
&w = M_\theta = N_{r\theta} = 0 \ \text{ at } \theta=0, \psi
\end{aligned} \tag{19}
$$

According to the thin sector plate formulation, the displacement field may be selected as

$$u = \sum_{i=1}^{\infty}\sum_{j=1}^{\infty} U_{ij}(t)\frac{\partial H_i(r)}{\partial r}R_j(\varphi) \tag{20}$$

$$v = \sum_{i=1}^{\infty}\sum_{j=1}^{\infty} V_{ij}(t)H_i(r)\frac{\partial R_j(\varphi)}{\partial \varphi} \tag{21}$$

$$w = \sum_{i=1}^{\infty}\sum_{j=1}^{\infty} W_{ij}(t)H_i(r)R_j(\varphi) \tag{22}$$

$$w^* = \sum_{i=1}^{\infty}\sum_{j=1}^{\infty} W^*(t)H_i(r)R_j(\varphi) \tag{23}$$

where (U, V, W) are the displacements amplitudes; W^* is the imperfection amplitude and the functions H_i and R_j are the test functions which are selected as

$$H_i(r) = \sin\frac{i\pi(r-r_0)}{r_1-r_0}, \quad R_j(\varphi) = \sin\left(\frac{j\pi\varphi}{\psi}\right) \tag{24}$$

Arranging the governing equations as B_i (u, v, w, w^*)=0 with (i=1,2,3) and inserting field components presented as Eqs. (20)-(23) into B_i yields following equations with the use of Galerkin's technique

$$\int_{r_0}^{r_1}\int_0^{\psi} B_1\frac{\partial H_i(r)}{\partial r}R_j(\varphi) r dr d\varphi = 0 \tag{25}$$

$$\int_{r_0}^{r_1}\int_0^{\psi} B_2 H_i(r)\frac{\partial R_j(\varphi)}{\partial \varphi} r dr d\varphi = 0 \tag{26}$$

$$\int_{r_0}^{r_1}\int_0^{\psi} B_3 H_i(r)R_j(\varphi) r dr d\varphi = 0 \tag{27}$$

Table 1 Material properties of the nanoparticle reinforced composite

	Epoxy	GOP	SiO_2
E (GPa)	3.45	444.8	74.8
v	0.35	0.165	0.19
ρ (kg/m^3)	1270	1090	2650

Table 2 Comparison of post-buckling loads of ideal and imperfect plates for various normalized amplitude.

$\tilde{W}/h$	W^*/h=0		W^*/h=0.1	
	Chikh *et al.* (2016)	present	Chikh *et al.* (2016)	present
0	0.62411	0.62411	0	0
0.1	0.62627	0.62627	0.31853	0.31853
0.2	0.63274	0.63274	0.43334	0.43334
0.3	0.64354	0.64354	0.50047	0.50047

After solving Eqs. (25)-(27) by neglecting in-plane inertias, three governing equations will be derived

$$S_{11}U + S_{21}V + S_{31}W + H_1W^2 + Y_1WW^* = 0 \tag{28}$$

$$S_{12}U + S_{22}V + S_{32}W + H_2W^2 + Y_2WW^* = 0 \tag{29}$$

$$
\begin{aligned}
&S_{13}U + S_{23}V + S_{33}W + H_3W^2 + H_4W^3 \\
&+H_5UW + H_6VW + Y_3WW^* \\
&+Y_4W^2W^* + Y_5W\left(W^*\right)^2 + Y_6UW^* \\
&+Y_7VW^* - P^*(W + W^*) = 0
\end{aligned} \tag{30}
$$

in which S_{ij} are linear stiffness matrix components; H_i denotes nonlinear stiffness components and Y_i are added stiffness due to geometric imperfection. Also, P^* denote the geometric matrix related to applied load. With the aid of Eqs. (28)-(30) one can express that

$$
\begin{aligned}
U &= \frac{S_{21}S_{32} - S_{22}(S_{31} + Y_1W^*)}{S_{11}S_{22} - S_{12}S_{21}}W + \frac{H_2S_{21} - H_1S_{22}}{S_{11}S_{22} - S_{12}S_{21}}W^2 \\
V &= \frac{S_{12}S_{31} - S_{11}(S_{32} + Y_2W^*)}{S_{11}S_{22} - S_{12}S_{21}}W + \frac{H_1S_{12} - H_2S_{11}}{S_{11}S_{22} - S_{12}S_{21}}W^2
\end{aligned} \tag{31}
$$

Then, applying Eq. (31) in Eq. (30) yields a single equation based on W and W^* only. The numerical solution of obtained equation for finding P_r will give post-buckling curves.

5. Discussion on results

In this section, post-buckling of a particle-reinforced annular sector plate modeled via nonlinear thin shell theory has been studied based upon provided solution approach. The dependency of post-buckling load $\tilde{P}_r = P_r/10^6 h$, on nanoparticles, inner/outer radius, normalized amplitude, geometric imperfectness and open angle will be explored. In this research, the material properties of nanoparticle reinforced annular plate are obtained when $d_{particle} =$

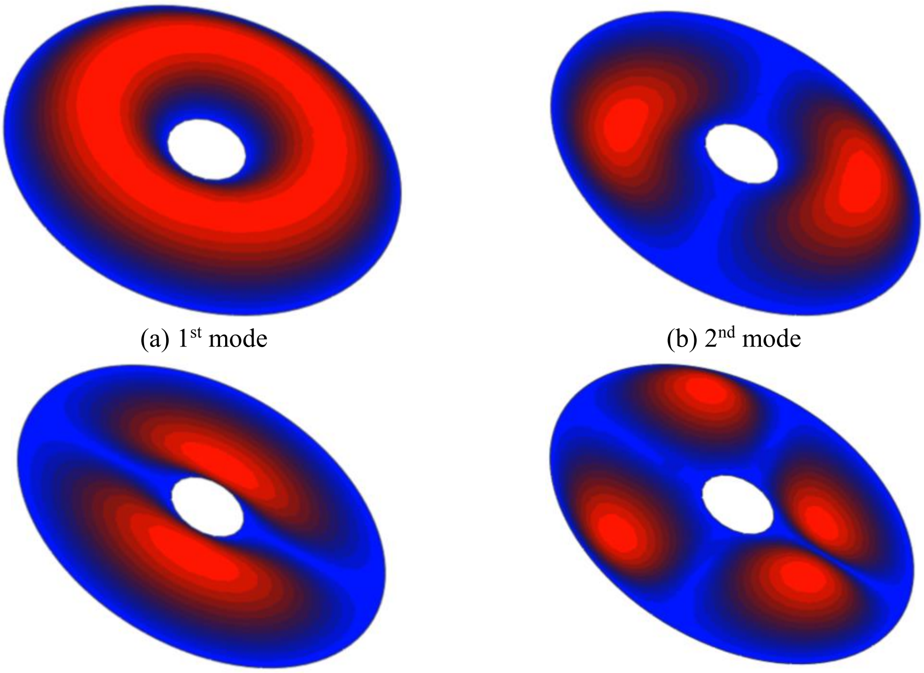

(a) 1st mode (b) 2nd mode

(c) 3rd mode (d) 4th mode

Fig. 2 First 4 mode shapes of GOP-reinforced annular plate (r_1/h=50, r_0=0.2r_1, $W_{particle}$=0.4%)

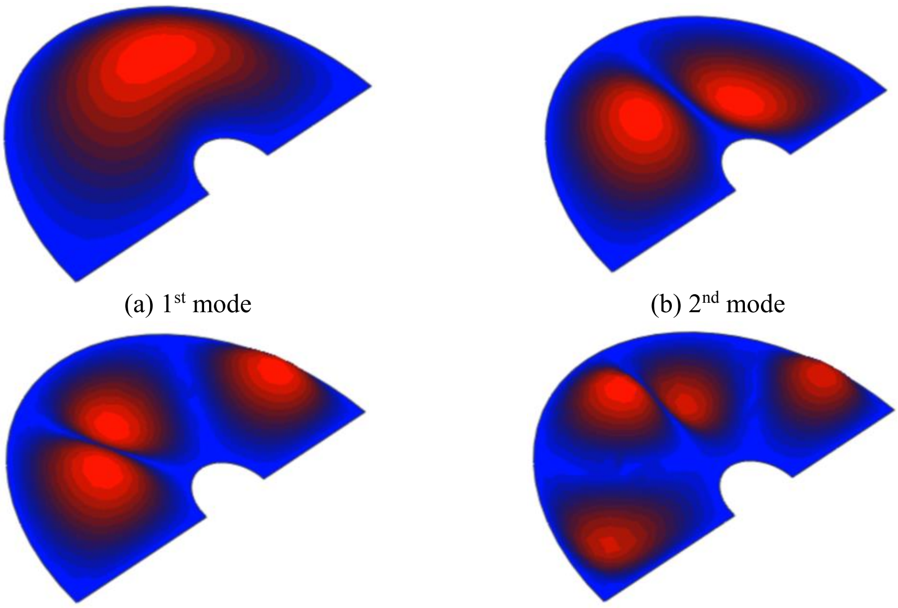

(a) 1st mode (b) 2nd mode

(c) 3rd mode (d) 4th mode

Fig. 3 First 4 mode shapes of GOP-reinforced annular sector (r_1/h=50, r_0=0.2r_1, ψ=π, $W_{particle}$=0.4%)

500 nm, $t_{particle} = 0.95$ nm . Also, Table 1 give the details of material proeprties for the matrix and nanoparticles. As the first step, post-buckling responses of perfect and imperfect square plates have been validated with those reported by Chikh *et al*. (2016) based on functionally graded (FG) plate model, as provided in Table 2. According to the table, buckling loads have been provided for both perfect (W^*/h=0) and imperfect (W^*/h=0.1) plates based on various normalized amplitude.

First four buckling mode shapes of nanoparticle reinforced annular plates are shown in Figs. 2 and 3 respectively for open angles of ψ=2π and ψ=π. The radius of annular plate is assumed to be r_1/h=50, r_0=0.2r_1. This figure gives a good insight about the buckling behavior of annular plates under compressive loads. Also, post-buckling load of graphene oxide particle-reinforced annular sector plate versus dimensionless deflection for different open angles is shown in Fig. 4. The figure shows that higher values for open angles result in lower post-buckling loads.

Influences of nanoparticle weight fraction ($W_{particle}$) on the post-buckling properties of annular plates are presented in Fig. 5 at imperfection amplitude of W^*/h=0.02. Uniform

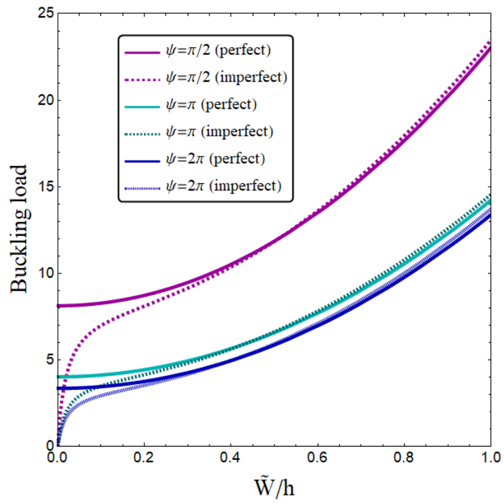

Fig. 4 Post-buckling load of graphene oxide particle-reinforced annular sector plate versus dimensionless deflection for different open angles (r_1/h=50, r_0=0.2r_1, $W_{particle}$=0.2%, W^*/h=0.02)

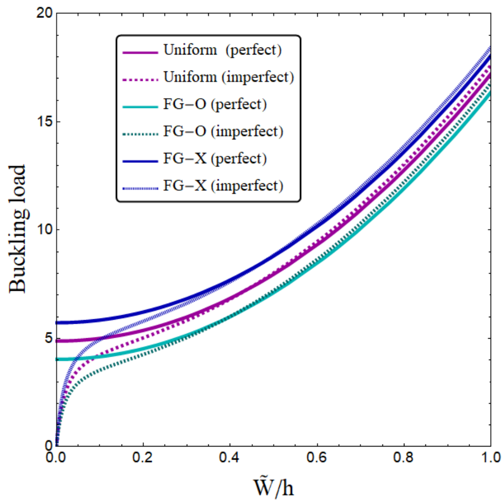

Fig. 6 Post-buckling load of graphene oxide particle-reinforced annular plate versus dimensionless deflection for different nanoparticle weight fractions ($W_{particle}$=0.4%, r_1/h=50, r_0=0.2r_1, ψ=π, W^*/h=0.02)

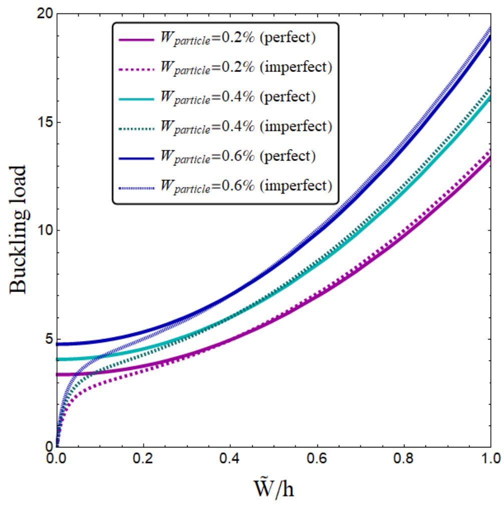

Fig. 5 Post-buckling load of graphene oxide particle-reinforced annular plate versus dimensionless deflection for different nanoparticle weight fractions (r_1/h=50, r_0=0.2r_1, ψ=2π, W^*/h=0.02)

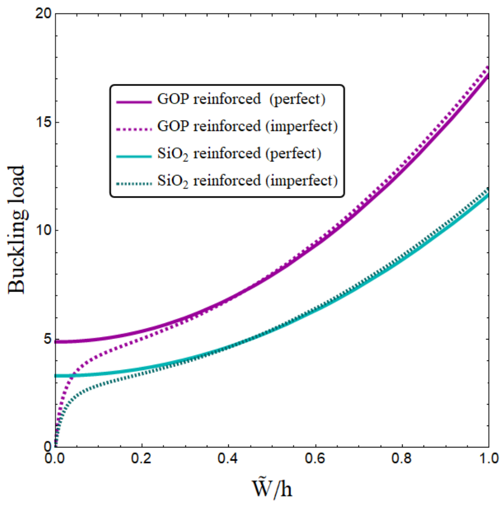

Fig. 7 Post-buckling load of graphene oxide particle-reinforced annular sector versus dimensionless deflection for different nanoparticle type (r_1/h=50, r_0=0.2r_1, ψ=π, $W_{particle}$=0.4%, W^*/h=0.02)

GOP distribution has been considered. In the case of ideal (perfect) annular plate, the load at $\tilde{W}/h=0$ is critical buckling load. However, in the case of imperfect annular plate ($W^*/h\neq0$), the critical buckling load does not exist, because the plate has an initial deflection. It must be pointed out that the buckling load becomes greater by increasing in normalized amplitude. The reason is intrinsic stiffening impact raised from geometric nonlinearity. Reinforcing effect of nanoparticles on mechanical properties of the plate is obviously observable from this graph. In fact, the effective stiffness of the reinforced annular plate may be prominently strengthened via adding a small amount of nanoparticles to matrix material.

In Fig. 6, post-buckling load-amplitude curves of a nanoparticle-reinforced annular plate with and without geometric imperfections have been presented accounting for various nanoparticle dispersions. It is considered that W^*=0.02h. The most important observation from this figure is that FG-X type of nanoparticle dispersion gives greater post-buckling loads than uniform and FG-O dispersions. As an outcome, controlling of nanoparticle is vital for obtaining the best mechanical performances of annular plates. Also, Fig. 7 presents post-buckling curves of the annular sector plate based on the two types of nanoparticles. According to this figure, using SiO_2 as reinforcing nanoparticle leads to smaller post-buckling loads compared to graphene as reinforcing nanoparticle.

Geometrical imperfection (W^*/h) effect on post-buckling behavior of nanoparticle-reinforced annular sector plate has been illustrated in Fig. 8. It may be observed that the initial deflection of plate has notable influences on the post-buckling load-deflection path. Based on previous

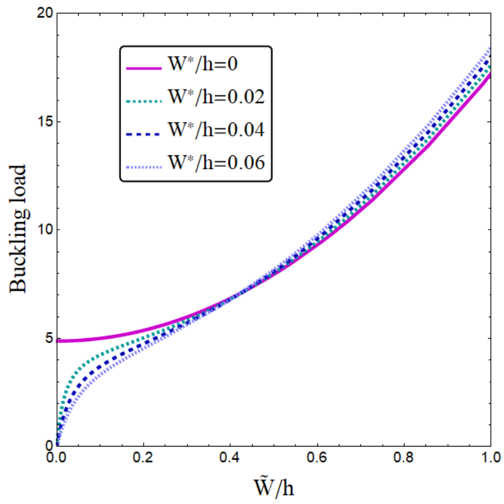

Fig. 8 Post-buckling load of GOP-reinforced annular sector versus dimensionless deflection for different geometric imperfections (ψ=π, $W_{particle}$=0.4%)

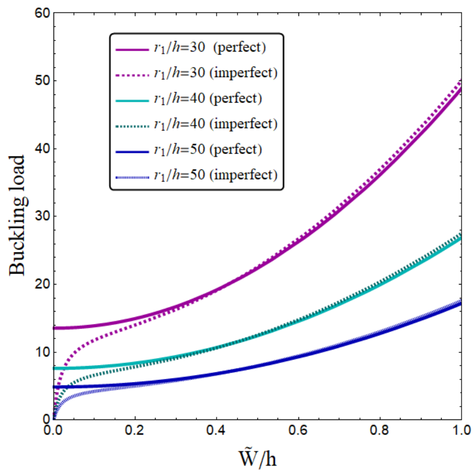

Fig. 9 Post-buckling load of graphene oxide particle-reinforced annular sector versus dimensionless deflection for different radius to thickness ratio (r_0=0.2r_1, ψ=π, $W_{particle}$=0.4%, W^*/h=0.02)

discussion, the critical buckling load vanishes by considering plate initial deflection. In fact, for the case of perfect structure (W^*/h=0), the plate has critical buckling. Next, plate buckling capacity improves by the increase of normalized deflection. However, for the case of imperfect structure ($W^*/h\neq0$), there is no buckling load before the initial situation of nanoparticle-reinforced annular plate. Thus, the buckling load is zero at the starting point for imperfect plates. After that, greater amplitudes of plates need stronger compressive load. Finally, it may be concluded that post-buckling curves of perfect and imperfect nanoparticle-reinforced annular plates become closer to each other at large values for normalized amplitude.

Effects of radius-to-thickness ratio (r_1/h) on post-buckling behaviors of nanoparticle-reinforced annular plates have been plotted in Fig. 9. Two cases of geometrically ideal (perfect) and imperfect plates have been supposed. It is obvious that nanoparticle-reinforced annular plates are less rigid at greater values for r_1/h. Accordingly, derived post-buckling load becomes lower via enlargement of r_1/h at prescribed normalized amplitudes ($\tilde{W}/h$). Also, calculated post-buckling loads for various values of r_1/h rely on the magnitude of normalized deflection. For smaller r_1/h, post-buckling load increases with a higher slope according to normalized deflection than higher radius-to-thickness ratio or thinner plates. Such observation is due to more stiffness of the annular plate at low values of r_1/h.

6. Conclusions

This article analyzed post-buckling behaviors of imperfect nanoparticle-reinforced annular plates via stablishing a nonlinear annular plate formulation in which geometric imperfection effects are involved. Uniform and functionally graded nanoparticle distributions were considered. Obtained findings in this research are presented as follows.

• Increasing nanoparticle weight fraction yields larger buckling loads. It means that adding the amount of nanoparticle can increase the plate stiffness and enhance its post-buckling behavior.
• FG-X nanoparticle distribution provided greater post-buckling loads than other distributions.
• An important finding was that as the magnitude of open angle is greater, the post-buckling load is lower.
• Using SiO_2 as reinforcing nanoparticle leads to smaller post-buckling loads compared to graphene as reinforcing nanoparticle.

Acknowledgement

The authors would like to thank FPQ (Fidar project Qaem) for providing the fruitful and useful help.

References

Abualnour, M., Chikh, A., Hebali, H., Kaci, A., Tounsi, A., Bousahla, A.A. and Tounsi, A. (2019), "Thermomechanical analysis of antisymmetric laminated reinforced composite plates using a new four variable trigonometric refined plate theory", *Comput. Concrete*, **24**(6), 489-498. https://doi.org/10.12989/cac.2019.24.6.489.

Addou, F.Y., Meradjah, M., Bousahla, A.A., Benachour, A., Bourada, F., Tounsi, A. and Mahmoud, S.R. (2019), "Influences of porosity on dynamic response of FG plates resting on Winkler/Pasternak/Kerr foundation using quasi 3D HSDT. *Comput. Concrete*, **24**(4), 347-367. https://doi.org/10.12989/cac.2019.24.4.347.

Ahankari, S.S. and Kar, K.K. (2010), "Hysteresis measurements and dynamic mechanical characterization of functionally graded natural rubber–carbon black composites", *Polym. Eng. Sci.*, **50**(5), 871-877. https://doi.org/10.1002/pen.21601.

Ahmed, R.A., Fenjan, R.M. and Faleh, N.M. (2019), "Analyzing post-buckling behavior of continuously graded FG nanobeams with geometrical imperfections", *Geomech. Eng.*, **17**(2), 175-180. https://doi.org/10.12989/gae.2019.17.2.175.

Al-Maliki, A.F., Faleh, N.M. and Alasadi, A.A. (2019), "Finite element formulation and vibration of nonlocal refined metal foam beams with symmetric and non-symmetric porosities", *Struct. Monit. Mainten.*, **6**(2), 147-159. https://doi.org/10.12989/smm.2019.6.2.147.

Alijani, M. and Bidgoli, M.R. (2018), "Agglomerated SiO2 nanoparticles reinforced-concrete foundations based on higher order shear deformation theory: Vibration analysis", *Adv. Concrete Constr.*, **6**(6), 585. https://doi.org/10.12989/acc.2018.6.6.585.

Alimirzaei, S., Mohammadimehr, M. and Tounsi, A. (2019), "Nonlinear analysis of viscoelastic micro-composite beam with geometrical imperfection using FEM: MSGT electro-magneto-elastic bending, buckling and vibration solutions", *Struct. Eng. Mech.*, **71**(5), 485-502. https://doi.org/10.12989/sem.2019.71.5.485.

Azimi, M., Mirjavadi, S.S., Shafiei, N. and Hamouda, A.M.S. (2017), "Thermo-mechanical vibration of rotating axially functionally graded nonlocal Timoshenko beam", *Appl. Phys. A*, **123**(1), 104. http://dx.doi.org/10.1007/s00339-017-0772-1.

Azimi, M., Mirjavadi, S.S., Shafiei, N., Hamouda, A.M.S. and Davari, E. (2018), "Vibration of rotating functionally graded Timoshenko nano-beams with nonlinear thermal distribution", *Mech. Adv. Mater. Struct.*, **25**(6), 467-480. https://doi.org/10.1080/15376494.2017.1285455.

Balubaid, M., Tounsi, A., Dakhel, B. and Mahmoud, S.R. (2019), "Free vibration investigation of FG nanoscale plate using nonlocal two variables integral refined plate theory", *Comput. Concrete*, **24**(6), 579-586. https://doi.org/10.12989/cac.2019.24.6.579.

Barati, M.R. (2017), "Nonlocal-strain gradient forced vibration analysis of metal foam nanoplates with uniform and graded porosities", *Adv. Nano Res.*, **5**(4), 393-414. https://doi.org/10.12989/anr.2017.5.4.393.

Barati, M.R. and Zenkour, A.M. (2018), "Analysis of postbuckling of graded porous GPL-reinforced beams with geometrical imperfection", *Mech. Adv. Mater. Struct.*, **26**(6), 503-511. https://doi.org/10.1080/15376494.2017.1400622.

Batou, B., Nebab, M., Bennai, R., Atmane, H.A., Tounsi, A. and Bouremana, M. (2019), "Wave dispersion properties in imperfect sigmoid plates using various HSDTs", *Steel Compos. Struct.*, **33**(5), 699. https://doi.org/10.12989/scs.2019.33.5.699.

Belbachir, N., Draich, K., Bousahla, A.A., Bourada, M., Tounsi, A. and Mohammadimehr, M. (2019), "Bending analysis of anti-symmetric cross-ply laminated plates under nonlinear thermal and mechanical loadings", *Steel Compos. Struct.*, **33**(1), 81-92. https://doi.org/10.12989/scs.2019.33.1.081.

Bellal, M., Hebali, H., Heireche, H., Bousahla, A. A., Tounsi, A., Bourada, F. and Tounsi, A. (2020), "Buckling behavior of a single-layered graphene sheet resting on viscoelastic medium via nonlocal four-unknown integral model", *Steel Compos. Struct.*, **34**(5), 643-655. https://doi.org/10.12989/scs.2020.34.5.643.

Berghouti, H., Adda Bedia, E.A., Benkhedda, A. and Tounsi, A. (2019), "Vibration analysis of nonlocal porous nanobeams made of functionally graded material", *Adv. Nano Res.*, **7**(5), 351-364. https://doi.org/10.12989/anr.2019.7.5.351.

Boukhlif, Z., Bouremana, M., Bourada, F., Bousahla, A.A., Bourada, M., Tounsi, A. and Al-Osta, M.A. (2019), "A simple quasi-3D HSDT for the dynamics analysis of FG thick plate on elastic foundation", *Steel Compos. Struct.*, **31**(5), 503-516. https://doi.org/10.12989/scs.2019.31.5.503.

Boulefrakh, L., Hebali, H., Chikh, A., Bousahla, A.A., Tounsi, A. and Mahmoud, S.R. (2019), "The effect of parameters of visco-Pasternak foundation on the bending and vibration properties of a thick FG plate", *Geomech. Eng.*, **18**(2), 161-178. https://doi.org/10.12989/gae.2019.18.2.161.

Bounouara, F., Benrahou, K.H., Belkorissat, I. and Tounsi, A. (2016), "A nonlocal zeroth-order shear deformation theory for free vibration of functionally graded nanoscale plates resting on elastic foundation", *Steel Compos. Struct.*, **20**(2), 227-249. https://doi.org/10.12989/scs.2016.20.2.227.

Bourada, F., Bousahla, A.A., Bourada, M., Azzaz, A., Zinata, A. and Tounsi, A. (2019), "Dynamic investigation of porous functionally graded beam using a sinusoidal shear deformation theory", *Wind Struct.*, **28**(1), 19-30. https://doi.org/10.12989/was.2019.28.1.019.

Boussoula, A., Boucham, B., Bourada, M., Bourada, F., Tounsi, A., Bousahla, A.A. and Tounsi, A. (2020). A simple nth-order shear deformation theory for thermomechanical bending analysis of different configurations of FG sandwich plates", *Smart Struct. Syst.*, **25**(2), 197. https://doi.org/10.12989/sss.2020.25.2.197.

Boutaleb, S., Benrahou, K.H., Bakora, A., Algarni, A., Bousahla, A.A., Tounsi, A. and Mahmoud, S.R. (2019), "Dynamic analysis of nanosize FG rectangular plates based on simple nonlocal quasi 3D HSDT", *Adv. Nano Res.*, **7**(3), 191. https://doi.org/10.12989/anr.2019.7.3.191.

Chaabane, L.A., Bourada, F., Sekkal, M., Zerouati, S., Zaoui, F.Z., Tounsi, A. and Tounsi, A. (2019), "Analytical study of bending and free vibration responses of functionally graded beams resting on elastic foundation", *Struct. Eng. Mech.*, **71**(2), 185-196. https://doi.org/10.12989/sem.2019.71.2.185.

Chikh, A., Bakora, A., Heireche, H., Houari, M.S.A., Tounsi, A. and Bedia, E.A. (2016), "Thermo-mechanical postbuckling of symmetric S-FGM plates resting on Pasternak elastic foundations using hyperbolic shear deformation theory", *Struct. Eng. Mech.*, **57**(4), 617-639. https://doi.org/10.12989/sem.2016.57.4.617.

Draiche, K., Bousahla, A.A., Tounsi, A., Alwabli, A.S., Tounsi, A. and Mahmoud, S.R. (2019), "Static analysis of laminated reinforced composite plates using a simple first-order shear deformation theory", *Comput. Concrete*, **24**(4), 369-378. https://doi.org/10.12989/cac.2019.24.4.369.

Draoui, A., Zidour, M., Tounsi, A. and Adim, B. (2019), "Static and dynamic behavior of nanotubes-reinforced sandwich plates using (FSDT)", *J. Nano Res.*, **57**, 117-135. https://doi.org/10.4028/www.scientific.net/JNanoR.57.117.

Du, H., Gao, H.J. and Dai Pang, S. (2016), "Improvement in concrete resistance against water and chloride ingress by adding graphene nanoplatelet", *Cement Concrete Res.*, **83**, 114-123. https://doi.org/10.1016/j.cemconres.2016.02.005.

Esawi, A.M.K., Morsi, K., Sayed, A., Taher, M and Lanka, S. (2011), "The influence of carbon nanotube (CNT) morphology and diameter on the processing and properties of CNT-reinforced aluminium composites", *Compos. Part A: Appl. Sci. Manuf.*, **42**(3), 234-243. https://doi.org/10.1016/j.compositesa.2010.11.008.

Faleh, N.M., Ahmed, R.A. and Fenjan, R.M. (2018), "On vibrations of porous FG nanoshells", *Int. J. Eng. Sci.*, **133**, 1-14. https://doi.org/10.1016/j.ijengsci.2018.08.007.

Fang, M., Wang, K., Lu, H., Yang, Y. and Nutt, S. (2009), "Covalent polymer functionalization of graphene nanosheets and mechanical properties of composites", *J. Mater. Chem.*, **19**(38), 7098-7105. https://doi.org/10.1039/B908220D.

Feng, C., Kitipornchai, S. and Yang, J. (2017). Nonlinear free vibration of functionally graded polymer composite beams reinforced with graphene nanoplatelets (GPLs)", *Eng. Struct.*, **140**, 110-119. https://doi.org/10.1016/j.engstruct.2017.02.052.

Fenjan, R.M., Ahmed, R.A., Alasadi, A.A. and Faleh, N.M. (2019), "Nonlocal strain gradient thermal vibration analysis of double-coupled metal foam plate system with uniform and non-uniform porosities", *Coupl. Syst. Mech.*, **8**(3), 247-257. https://doi.org/10.12989/csm.2019.8.3.247.

Gojny, F.H., Wichmann, M.H.G., Köpke, U., Fiedler, B. and Schulte, K. (2004), "Carbon nanotube-reinforced epoxy-composites: enhanced stiffness and fracture toughness at low nanotube content", *Compos. Sci. Technol.*, **64**(15), 2363-2371. https://doi.org/10.1016/j.compscitech.2004.04.002.

Guenaneche, B., Benyoucef, S., Tounsi, A. and Adda Bedia, E.A. (2019), "Improved analytical method for adhesive stresses in plated beam: Effect of shear deformation", *Adv. Concrete Constr.*, **7**(3), 151-166. https://doi.org/10.12989/acc.2019.7.3.151.

Hao, P., Wang, B., Du, K., Li, G., Tian, K., Sun, Y. and Ma, Y. (2016), "Imperfection-insensitive design of stiffened conical shells based on equivalent multiple perturbation load approach", *Compos. Struct.*, **136**, 405-413. https://doi.org/10.1016/j.compstruct.2015.10.022.

Hellal, H., Bourada, M., Hebali, H., Bourada, F., Tounsi, A., Bousahla, A.A. and Mahmoud, S.R. (2019), "Dynamic and stability analysis of functionally graded material sandwich plates in hygro-thermal environment using a simple higher shear deformation theory", *J. Sandw. Struct. Mater.*, 1099636219845841. https://doi.org/10.1177%2F1099636219845841.

Hussain, M., Naeem, M.N., Tounsi, A. and Taj, M. (2019), "Nonlocal effect on the vibration of armchair and zigzag SWCNTs with bending rigidity", *Adv. Nano Res.*, **7**(6), 431. https://doi.org/10.12989/anr.2019.7.6.431.

Kaddari, M., Kaci, A., Bousahla, A.A., Tounsi, A., Bourada, F., Bedia, E.A. and Al-Osta, M.A. (2020), "A study on the structural behaviour of functionally graded porous plates on elastic foundation using a new quasi-3D model: bending and free vibration analysis", *Comput. Concrete*, **25**(1), 37. https://doi.org/10.12989/cac.2020.25.1.037.

Keleshteri, M.M., Asadi, H. and Wang, Q. (2017), "Large amplitude vibration of FG-CNT reinforced composite annular plates with integrated piezoelectric layers on elastic foundation", *Thin Wall. Struct.*, **120**, 203-214. https://doi.org/10.1016/j.tws.2017.08.035.

King, J.A., Klimek, D.R., Miskioglu, I. and Odegard, G.M. (2013), "Mechanical properties of graphene nanoplatelet/epoxy composites", *J. Appl. Polym. Sci.*, **128**(6), 4217-4223. https://doi.org/10.1002/app.38645.

Kitipornchai, S., Chen, D. and Yang, J. (2017), "Free vibration and elastic buckling of functionally graded porous beams reinforced by graphene platelets", *Mater. Des.*, **116**, 656-665. https://doi.org/10.1016/j.matdes.2016.12.061.

Lal, A. and Markad, K. (2018), "Deflection and stress behaviour of multi-walled carbon nanotube reinforced laminated composite beams", *Comput. Concrete*, **22**(6), 501-514. https://doi.org/10.12989/cac.2018.22.6.501.

Liew, K.M., Lei, Z.X. and Zhang, L.W. (2015), "Mechanical analysis of functionally graded carbon nanotube reinforced composites: a review", *Compos. Struct.*, **120**, 90-97. https://doi.org/10.1016/j.compstruct.2014.09.041.

Lin, F., Yang, C., Zeng, Q.H and Xiang, Y. (2018), "Morphological and mechanical properties of graphene-reinforced PMMA nanocomposites using a multiscale analysis", *Comput. Mater. Sci.*, **150**, 107-120.

Mahmoudi, A., Benyoucef, S., Tounsi, A., Benachour, A., Adda Bedia, E.A. and Mahmoud, S.R. (2019), "A refined quasi-3D shear deformation theory for thermo-mechanical behavior of functionally graded sandwich plates on elastic foundations", *J. Sandw. Struct. Mater.*, **21**(6), 1906-1929. https://doi.org/10.1177%2F1099636217727577.

Medani, M., Benahmed, A., Zidour, M., Heireche, H., Tounsi, A., Bousahla, A.A. and Mahmoud, S.R. (2019), "Static and dynamic behavior of (FG-CNT) reinforced porous sandwich plate using energy principle", *Steel Compos. Struct.*, **32**(5), 595-610. https://doi.org/10.12989/scs.2019.32.5.595.

Meksi, R., Benyoucef, S., Mahmoudi, A., Tounsi, A., Adda Bedia, E.A. and Mahmoud, S.R. (2019), "An analytical solution for bending, buckling and vibration responses of FGM sandwich plates", *J. Sandw. Struct. Mater.*, **21**(2), 727-757. https://doi.org/10.1177%2F1099636217698443.

Metwally, I.M. (2014), "Three-dimensional finite element analysis of reinforced concrete slabs strengthened with epoxy-bonded steel plates", *Adv. Concrete Constr.*, **2**(2), 91. https://doi.org/10.12989/acc.2014.2.2.091.

Mirjavadi, S.S., Afshari, B.M., Barati, M.R. and Hamouda, A.M.S. (2018), "Strain gradient based dynamic response analysis of heterogeneous cylindrical microshells with porosities under a moving load", *Mater. Res. Exp.*, **6**(3), 035029.

Mirjavadi, S.S., Afshari, B.M., Barati, M.R. and Hamouda, A.M.S. (2019), "Transient response of porous FG nanoplates subjected to various pulse loads based on nonlocal stress-strain gradient theory", *Eur. J. Mech.-A/Solid.*, **74**, 210-220. https://doi.org/10.1016/j.euromechsol.2018.11.004.

Mirjavadi, S.S., Afshari, B.M., Barati, M.R. and Hamouda, A.M.S. (2019), "Nonlinear free and forced vibrations of graphene nanoplatelet reinforced microbeams with geometrical imperfection", *Microsyst. Technol.*, **25**, 3137–3150. https://doi.org/10.1007/s00542-018-4277-4.

Mirjavadi, S.S., Afshari, B.M., Khezel, M., Shafiei, N., Rabby, S. and Kordnejad, M. (2018), "Nonlinear vibration and buckling of functionally graded porous nanoscaled beams", *J. Brazil. Soc. Mech. Sci. Eng.*, **40**(7), 352. https://doi.org/10.1007/s00542-018-4277-4.

Mirjavadi, S.S., Afshari, B.M., Shafiei, N., Hamouda, A.M.S. and Kazemi, M. (2017), "Thermal vibration of two-dimensional functionally graded (2D-FG) porous Timoshenko nanobeams", *Steel Compos. Struct.*, **25**(4), 415-426. https://doi.org/10.12989/scs.2017.25.4.415.

Mirjavadi, S.S., Forsat, M., Barati, M.R., Abdella, G.M., Afshari, B.M., Hamouda, A.M.S. and Rabby, S. (2019), "Dynamic response of metal foam FG porous cylindrical micro-shells due to moving loads with strain gradient size-dependency", *Eur. Phys. J. Plus*, **134**(5), 214. https://doi.org/10.1140/epjp/i2019-12540-3.

Mirjavadi, S.S., Forsat, M., Barati, M.R., Abdella, G.M., Hamouda, A.M.S., Afshari, B.M. and Rabby, S. (2019), "Post-buckling analysis of piezo-magnetic nanobeams with geometrical imperfection and different piezoelectric contents", *Microsyst. Technol.*, **25**(9), 3477-3488. https://doi.org/10.1007/s00542-018-4241-3.

Mirjavadi, S.S., Forsat, M., Hamouda, A.M.S. and Barati, M.R. (2019), "Dynamic response of functionally graded graphene nanoplatelet reinforced shells with porosity distributions under transverse dynamic loads", *Mater. Res. Exp.*, **6**(7), 075045.

Mirjavadi, S.S., Forsat, M., Nikookar, M., Barati, M.R. and Hamouda, A.M.S. (2019), "Nonlinear forced vibrations of sandwich smart nanobeams with two-phase piezo-magnetic face sheets", *Eur. Phys. J. Plus*, **134**(10), 508. https://doi.org/10.1140/epjp/i2019-12806-8.

Mirjavadi, S.S., Rabby, S., Shafiei, N., Afshari, B.M. and Kazemi, M. (2017), "On size-dependent free vibration and thermal buckling of axially functionally graded nanobeams in thermal environment", *Appl. Phys. A*, **123**(5), 315. https://doi.org/10.1007/s00339-017-0918-1.

Mohammed, A., Sanjayan, J.G., Nazari, A. and Al-Saadi, N.T.K. (2017), "Effects of graphene oxide in enhancing the performance of concrete exposed to high-temperature", *Aust. J. Civil Eng.*, **15**(1), 61-71. https://doi.org/10.1080/14488353.2017.1372849.

Mouffoki, A., Bedia, E.A., Houari, M.S.A., Tounsi, A. and Mahmoud, S.R. (2017), "Vibration analysis of nonlocal advanced nanobeams in hygro-thermal environment using a new two-unknown trigonometric shear deformation beam theory", *Smart Struct. Syst.*, **20**(3), 369-383. https://doi.org/10.12989/sss.2017.20.3.369.

Nieto, A., Bisht, A., Lahiri, D., Zhang, C. and Agarwal, A. (2017), "Graphene reinforced metal and ceramic matrix composites: a review", *Int. Mater. Rev.*, **62**(5), 241-302. https://doi.org/10.1080/09506608.2016.1219481.

Rafiee, M.A., Rafiee, J., Wang, Z., Song, H., Yu, Z.Z. and Koratkar, N. (2009), "Enhanced mechanical properties of nanocomposites at low graphene content", *ACS Nano*, **3**(12), 3884-3890. https://doi.org/10.1021/nn9010472.

Rezaiee-Pajand, M., Masoodi, A.R. and Mokhtari, M. (2018), "Static analysis of functionally graded non-prismatic sandwich beams", *Adv. Comput. Des.*, **3**(2), 165-190. https://doi.org/10.12989/acd.2018.3.2.165.

Sahla, M., Saidi, H., Draiche, K., Bousahla, A.A., Bourada, F. and Tounsi, A. (2019), "Free vibration analysis of angle-ply laminated composite and soft core sandwich plates", *Steel Compos. Struct.*, **33**(5), 663. https://doi.org/10.12989/scs.2019.33.5.663.

Semmah, A., Heireche, H., Bousahla, A.A. and Tounsi, A. (2019), "Thermal buckling analysis of SWBNNT on Winkler foundation by non local FSDT", *Adv. Nano Res.*, **7**(2), 89. https://doi.org/10.12989/anr.2019.7.2.089.

Shafiei, N., Mirjavadi, S.S., Afshari, B.M., Rabby, S. and Hamouda, A.M.S. (2017), "Nonlinear thermal buckling of axially functionally graded micro and nanobeams", *Compos. Struct.*, **168**, 428-439. https://doi.org/10.1016/j.compstruct.2017.02.048.

Shamsaei, E., de Souza, F.B., Yao, X., Benhelal, E., Akbari, A. and Duan, W. (2018), "Graphene-based nanosheets for stronger and more durable concrete: A review", *Constr. Build. Mater.*, **183**, 642-660. https://doi.org/10.1016/j.conbuildmat.2018.06.201.

Shen, H.S., Xiang, Y., Lin, F. and Hui, D. (2017), "Buckling and postbuckling of functionally graded graphene-reinforced composite laminated plates in thermal environments", *Compos. Part B: Eng.*, **119**, 67-78. https://doi.org/10.1016/j.compositesb.2017.03.020.

Song, M., Kitipornchai, S. and Yang, J. (2017), "Free and forced vibrations of functionally graded polymer composite plates reinforced with graphene nanoplatelets", *Compos. Struct.*, **159**, 579-588. https://doi.org/10.1016/j.compstruct.2016.09.070.

Tlidji, Y., Zidour, M., Draiche, K., Safa, A., Bourada, M., Tounsi, A. and Mahmoud, S.R. (2019), "Vibration analysis of different material distributions of functionally graded microbeam", *Struct. Eng. Mech.*, **69**(6), 637-649. https://doi.org/10.12989/sem.2019.69.6.637.

Wang, B., Zhu, S., Hao, P., Bi, X., Du, K., Chen, B. and Chao, Y.J. (2018), "Buckling of quasi-perfect cylindrical shell under axial compression: a combined experimental and numerical investigation", *Int. J. Solid. Struct.*, **130**, 232-247. https://doi.org/10.1016/j.ijsolstr.2017.09.029.

Wang, L. and Su, R.K.L. (2013), "A unified design procedure for preloaded rectangular RC columns strengthened with post-compressed plates", *Adv. Concrete Constr.*, **1**(2), 163. https://doi.org/10.12989/acc.2013.1.2.163.

Yang, B., Yang, J. and Kitipornchai, S. (2017), "Thermoelastic analysis of functionally graded graphene reinforced rectangular plates based on 3D elasticity", *Meccanica*, **52**(10), 2275-2292. https://doi.org/10.1007/s11012-016-0579-8.

Zaheer, M.M., Jafri, M.S. and Sharma, R. (2019), "Effect of diameter of MWCNT reinforcements on the mechanical properties of cement composites", *Adv. Concrete Constr.*, **8**(3), 207-215. https://doi.org/10.12989/acc.2019.8.3.207.

Zaoui, F.Z., Ouinas, D. and Tounsi, A. (2019), "New 2D and quasi-3D shear deformation theories for free vibration of functionally graded plates on elastic foundations", *Compos. Part B: Eng.*, **159**, 231-247. https://doi.org/10.1016/j.compositesb.2018.09.051.

Zaoui, F.Z., Tounsi, A., Ouinas, D. and Olay, J.A.V. (2020), "A refined HSDT for bending and dynamic analysis of FGM plates", *Struct. Eng. Mech.*, **74**(1), 105-119. https://doi.org/10.12989/sem.2020.74.1.105.

Zarga, D., Tounsi, A., Bousahla, A.A., Bourada, F. and Mahmoud, S.R. (2019), "Thermomechanical bending study for functionally graded sandwich plates using a simple quasi-3D shear deformation theory", *Steel Compos. Struct.*, **32**(3), 389-410. https://doi.org/10.12989/scs.2019.32.3.389.

Zemri, A., Houari, M.S.A., Bousahla, A.A. and Tounsi, A. (2015), "A mechanical response of functionally graded nanoscale beam: an assessment of a refined nonlocal shear deformation theory beam theory", *Struct. Eng. Mech.*, **54**(4), 693-710. https://doi.org/10.12989/sem.2015.54.4.693.

Zhang, L.W. (2017), "On the study of the effect of in-plane forces on the frequency parameters of CNT-reinforced composite skew plates", *Compos. Struct.*, **160**, 824-837. https://doi.org/10.1016/j.compstruct.2016.10.116.

Zhang, Z., Li, Y., Wu, H., Zhang, H., Wu, H., Jiang, S. and Chai, G. (2020), "Mechanical analysis of functionally graded graphene oxide-reinforced composite beams based on the first-order shear deformation theory", *Mech. Adv. Mater. Struct.*, **27**, 3-11. https://doi.org/10.1080/15376494.2018.1444216.

CC